JOURNAL OF CATALYSIS **170,** 275–285 (1997)
ARTICLE NO. CA971767

Electrochemical Promotion of the Catalytic Reduction of NO by CO on Palladium

M. Marwood and C. G. Vayenas[1]

Department of Chemical Engineering, University of Patras, Patras GR-26500, Greece

Received July 23, 1996; revised May 19, 1997; accepted June 2, 1997

It was found that the catalytic activity and selectivity of Pd for the reduction of NO by CO at temperatures of 600 to 750 K can be markedly and reversibly affected by depositing a polycrystalline Pd film on 8 mol% Y_2O_3-stabilized-ZrO_2 (YSZ), an O^{2-} conductor, and applying external negative currents or potentials between the catalyst and a Au counter electrode. The increase in the rate of reduction of NO is typically more than 700 times larger than the rate of removal of O^{2-} from the catalyst via negative current application, while the CO_2 and N_2 formation rates can be respectively doubled and tripled. The promotional effect is explained by an enhanced dissociation of NO on the Pd surface which is moderated by a stronger adsorption of CO relative to NO. The $N_2O + CO$ reaction was also studied and exhibited a twofold enhancement of the rate, in the most favorable cases, as negative or positive potentials or currents were applied. It was concluded that this reaction is not an important route to the formation of N_2 during the NO + CO reaction under these conditions.

INTRODUCTION

Considerable research effort has recently been focused on finding materials capable of replacing or diminishing the use of costly Rh in three-way catalysts. The metallic active component the most commonly mentioned is Pd, which is closer to Rh than Pt and is considerably less expensive (e.g., (1–5)). The main disadvantage of Pd, relative to the conventional Rh/Pt catalyst lies in its poorer NO_x reduction ability, as well as in a narrower air/fuel ratio window for high NO_x conversions. It is therefore of technological interest to find means of enhancing the NO_x performance of Pd. The use of additives, such as MoO_3 (6) or La_2O_3 (7, 8) was shown to improve significantly the activity and selectivity of Pd for converting NO to N_2 and to result in catalysts exhibiting performance characteristics almost similar to that of the Rh catalyst. The present work addresses the effect of electrochemical promotion on the Pd-catalyzed NO reduction by CO.

Non-Faradaic electrochemical modification of catalyst activity (NEMCA) or electrochemical promotion is now a well-established effect that has been observed for 40 different catalytic reactions over a wide range of different metals. Work in this area has been extensively reviewed (9, 10). In brief it has been found that the catalytic and chemisorptive properties of polycrystalline metal films interfaced with solid electrolytes, such as yttria-stabilized-zirconia (YSZ), an O^{2-} conductor, β''-Al_2O_3, a Na^+ conductor, CaF_2, a F^- conductor, or TiO_2, a mixed electronic–ionic conductor, can be affected dramatically and reversibly by electrically polarizing the metal–solid electrolyte interface. It was recently found that the use of β''-Al_2O_3 to reversibly dose Na on Pt leads to very significant enhancement in the rate and N_2 selectivity of the Pt-catalyzed NO reduction by CO (11), C_2H_4 (12), C_3H_6 (13), and H_2 (14).

One of the distinctive features of Pd and Pt, as compared to Rh, is their less facile dissociation of NO (2). The dissociative adsorption of NO on Pd is strongly structure sensitive (15) and is favored by stepped sites (16–18). The degree of dissociation is shown to depend both on the temperature and coverage of NO. High coverages of NO inhibit the dissociation. NO adsorbs molecularly on Pd at room temperature, while dissociation of NO is reported for single crystals and supported catalysts at temperatures larger than 500 K (16–23). TPD experiments of CO (22) showed that the order of strength of CO adsorption is Pt > Pd > Rh. Whereas on Pt, carbonyl complexes prohibit the formation of nitrosil species and replace them from the surface, these complexes were shown by *in situ* infrared spectroscopy to coexist on Pd and Rh supported on γ-Al_2O_3 at temperatures up to 473 K and a composition of 0.9% NO + 1.3% CO (24–25). Mixed overlayers of adsorbed CO and NO are proposed for Pd(100) under vacuum conditions and temperatures of CO + NO adsorption of 100 K (26) and 100 to 500 K (27). NO appears to better compete with O_2 for CO over Rh than over Pd since the addition of NO inhibits the CO + O_2 reaction over Rh but not over Pd (28). This behavior is thought to reflect a higher N atom concentration on the Rh than on the Pd surface, adsorbed N inhibiting the adsorption of O_2 (2). A low N surface coverage (N/Pd = 0.02) is measured by Yamada *et al.* (23) by AES after exposing Pd(100) to 1 Torr of CO and 1 Torr of NO at 600 K.

[1] To whom correspondence should be addressed.

0021-9517/97 $25.00

Relatively few kinetic studies pertaining to the reduction of NO by CO on Pd can be found in the literature. Butler and Davis (29) and Muraki *et al.* (30) measured a negative-order dependence on CO partial pressure and a second- or first-order dependence on NO partial pressure for Pd supported on Al_2O_3 at 573–723 K and 623 K, respectively. A Langmuir–Hinshelwood type kinetic behavior with P_{NO} is measured by Papadakis *et al.* (5) at 633 K for Pd supported on various supports. Activation energies in the range of 85 to 91 kJ/mol are reported for different systems and pressures (28, 29, 31) with the exception of values of 58 kJ/mol ($T < 470$ K) and 140 kJ/mol ($T > 470$ K) reported by Bogdanchikova *et al.* (32). A reaction scheme involving the dissociative adsorption of NO is proposed by several authors (30, 32) while a bimolecular scheme, where NO and CO react without prior dissociation of NO, is proposed by others (16, 29, 31).

This paper is the first study of electrochemical promotion of the NO reduction on Pd. Carbon monoxide is used as the reductant and yttria-stabilized-zirconia (YSZ) as the solid electrolyte support of the Pd catalyst film. The choice of this material rather than β''-Al_2O_3 was dictated by the fact that YSZ is already used in car exhaust systems as the major component of the oxygen sensor and its long-term stability under operation is known. Results for the N_2O reduction by CO are also reported since several studies performed on Rh (33–35) and Pt (36–37) have shown that N_2O formed during the NO + CO reaction could undergo further reaction with CO to produce N_2 and CO_2.

EXPERIMENTAL

The YSZ disk was suspended in a quartz continuous flow well-mixed reactor with all three electrodes exposed to the reactant gas mixture (Fig. 1). The quartz reactor volume was 25 cm^3 and the performance of this type of single pellet CSTR has been described and discussed elsewhere (9, 38). On-line gas chromatography was used for analysis of reactants and products. The separation of CO_2 and N_2O was performed on a Porapaq Q column at 313 K while CO and NO were separated using a Molecular Sieve 5A packed column at 373 K. CO_2 was also continuously monitored with an IR analyzer (ANARAD AR-500). The carbon and oxygen mass balance was found to close within 2%. Quoted N_2 rates (r_{N_2}) were computed from the measured CO_2 and N_2O rates via:

$$r_{N_2} = 0.5(r_{CO_2} - r_{N_2O}), \quad [1]$$

according to the following stoichiometric equations:

$$NO + CO \rightarrow CO_2 + 0.5N_2 \quad [2]$$

$$2NO + CO \rightarrow CO_2 + N_2O. \quad [3]$$

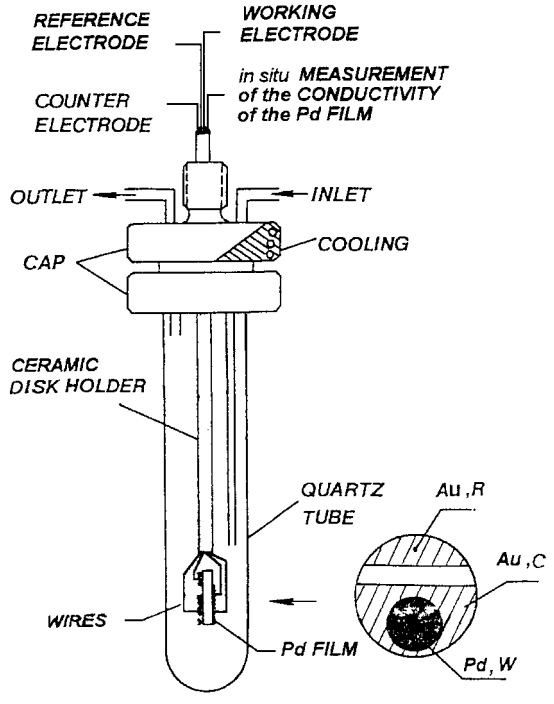

FIG. 1. Single pellet catalytic reactor and electrode configuration.

The selectivity towards nitrogen S_{N_2} was computed via

$$S_{N_2} = r_{N_2}/(r_{N_2} + r_{N_2O}) = (r_{CO_2} - r_{N_2O})/(r_{CO_2} + r_{N_2O}). \quad [4]$$

The catalytic rate measurements under potentiostatic or galvanostatic conditions were carried out using a galvanostat-potentiostat (Amel type 553). The current interruption technique (9, 10) was used to obtain the ohmic-drop-free catalyst potential V_{WR} from the raw catalyst potential V'_{WR} data.

The reactant gas mixture was delivered at total flowrates of 200–300 Nml/min, with partial pressures P_{NO}, P_{CO}, P_{N_2O} varied between 0–1.6, 0–1.0, and 0–6.0 kPa, respectively, and with P_{He}, giving a total pressure of 1 atm in every case. Conversion of the reactants was always below 15%. CO was passed through a heated quartz trap at 523 K to eliminate possible contamination by Fe carbonyl. Control experiments confirmed that the Au reference and counterelectrodes were catalytically inert under all conditions.

Preparation of the Pd Film

Gold reference and counterelectrodes were deposited on one side of a YSZ disk (Didier Werke AG; diameter 19 mm; thickness 3 mm) by using a Au paste prepared by mixing Aldrich Au powder (99.9%+) in a slurry of polyvinyl acetate binder in ethyl acetate, followed by calcination at 1173 K for 2 h. The catalyst (working electrode) consisted of a thin Pd film deposited on the other side of the YSZ disk by using a thin coating of Engelhard A1122 paste calcined

in air at 723 K for 6 h. The sample was then mounted in the reactor and reduced *in situ* at 333 K in a flow of 60 Nml/min of 2% H_2 in He for 30 min. Two gold wires were pressed on the surface of the film and allowed to measure *in situ* the resistance of the Pd film and, thus, to follow the extent of the reduction. An abrupt decrease of the resistance from the initial value of 10 kΩ to 5 Ω was observed at 333 K. The catalyst was further heated to 573 K in the reducing mixture for 2 h to ensure complete reduction of the film. Subsequently the catalyst was exposed to the reacting gas mixture ($P_{CO} = 0.55$ kPa, $P_{NO} = 1.3$ kPa, balance He) at 723 K and the rates of N_2, N_2O, and CO_2 formation were monitored as a function of time. During this catalyst aging period the catalyst activity was found to gradually increase by up to 50% until, after a week on stream, steady-state and reproducible performance was reached. All results reported here were obtained after the catalyst had reached this steady and reproducible performance which did not change until the end of the kinetic and electrokinetic investigation a few months later. Upon removal of the YSZ disk from the reactor after the end of the experiments, it was noticed that reduction and reaction had caused a change in the texture of the Pd film, relative to its initial prereduced state, also evidenced by optical microscopy, as the film had obtained a lighter gray metallic color.

The Pd catalyst film was characterized by measuring it surface area (39) *after* it had reached steady-state catalytic performance. The surface area was measured via surface titration of CO by oxygen at 623 K, following the technique described by Stoukides and Vayenas (39). In brief, CO was allowed to chemisorb *in situ* on the Pd surface, followed by exposure to a stream of ultrapure He for a time, t_{He}, at least 8 times longer than the residence time of the CSTR. Subsequently the catalyst film was exposed to a stream of synthetic air and the mass of CO adsorbed at t_{He} was found by integrating, via the IR CO_2 analyzer, the area of the CO_2 peak formed by reaction of adsorbed CO with oxygen. By varying t_{He} one can study the kinetics of CO desorption (Fig. 2). By extrapolating to $t_{He} = 0$ one can obtain the maximum reactive CO uptake of the catalyst, N_O (Fig. 2). This gave a value of 0.91 μmol of Pd for the active sites (Fig. 2) assuming a 1 : 1 stoichiometry for CO chemisorption on Pd. This value ($N_O = 0.91$ μmol) was used to express, when desired, measured rate values into turnover frequencies (TOF, s^{-1}).

Different methods of preparing a conductive Pd film were tested prior to the one described above. The technique which consists of calcining the Engelhard Pd paste at high temperatures in order to first decompose the organics contained in the paste, to form a metal oxide, and to disproportionate this oxide to obtain the metal was not successful, as a nonconductive film of PdO was always obtained. Calcining the sample to temperatures as high as 1373 K did not result in the decomposition of the PdO even though bulk thermodynamics predict the disproportionation of the oxide at 1073 K (40). The film thus formed exhibited a resistance higher than 20 MΩ. The stabilization of the oxide has been observed by different authors, who attribute it tentatively to a strong interaction with the oxide support material (41) or to the formation of a cluster oxide phase (40). The *in situ* reduction of the film of PdO in 2% H_2 resulted in the desegregation of the film to a powder, which can be explained by the fact that PdO has a volume 1.5 times that of Pd (42). The calcination temperature of 723 K used for the preparation of the conductive catalyst was chosen so that organics of the paste would be fully oxidized but no bulk Pd oxide would form. This appears to be important for the deposition of conductive and well-adhered Pd films on YSZ.

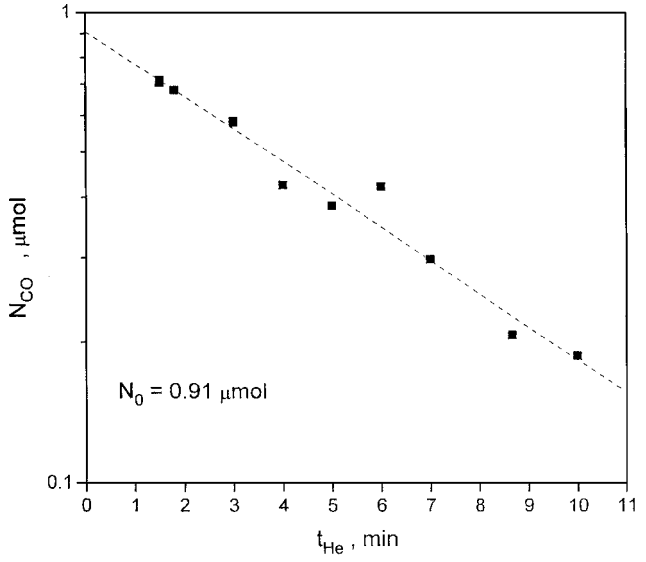

FIG. 2. Surface titration of CO by oxygen: Effect of desorption time, t_{He}, on the amount of CO adsorbed on the Pd surface.

RESULTS

Galvanostatic Transient

A galvanostatic transient experiment is shown in Fig. 3, where the response of the overall reaction rate r_{CO_2} and catalyst potential V'_{WR} are plotted as a function of time upon the application of a constant current $I = -10$ μA. Initially ($t < 0$), the circuit is open ($I = 0$, $V'_{WR} = -0.236$ V) and the catalytic rate $r^0_{CO_2}$ is 4.0×10^{-8} mol/s. The corresponding turnover frequency (TOF) is 0.044 s^{-1}. At $t = 0$, the galvanostat is used to apply a constant current $I = -10$ μA between the catalyst and the counterelectrode; O^{2-} ions are transported from the catalyst to the counterelectrode at a rate $I/2F = 5.2 \times 10^{-11}$ mol O/s. The overall catalytic rate increases by a factor of two to reach a new steady-state value $r_{CO_2} = 7.8 \times 10^{-8}$ mol/s and $V'_{WR} = -1.824$ V in approximately 60 min. The new TOF is 0.086 s^{-1}. The increase

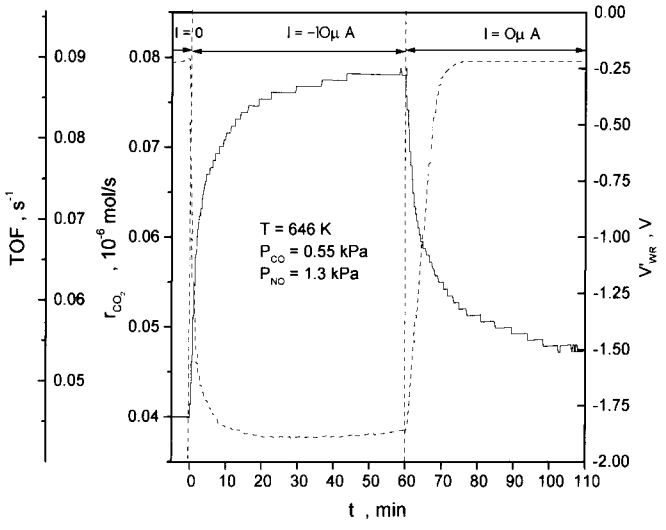

FIG. 3. Galvanostatic transient showing the effect of a step change of the applied current ($I = -10\,\mu A$) on the CO_2 formation (solid line) and on the catalyst potential V'_{WR} (dotted line) as a function of time. Conditions: $T = 646$ K, $P^0_{NO} = 1.30$ kPa, $P^0_{CO} = 0.55$ kPa.

in the catalytic rate $\Delta r_{CO_2} = r - r^0 = 3.8 \times 10^{-8}$ mol/s is 730 times larger than the rate of O^{2-} transport to the counterelectrode and thus the effect is non-Faradaic (NEMCA effect). Upon current interruption, the catalytic rate r_{CO_2} and V'_{WR} tend to relax to their open-circuit value.

Effect of the Catalyst Potential and Work Function

In Fig. 4, the steady-state rates for CO_2, N_2, and N_2O production, as well as the selectivity for nitrogen, S_{N_2}, are presented as a function of the ohmic-drop-free potential V_{WR} (9) at 646 K for a constant inlet pressure of the reactants $P^0_{NO} = 1.34$ kPa and $P^0_{CO} = 0.55$ kPa. Steady-state open-circuit conditions were attained before the application of each different value of the potential. The top axis of the figure is based on the equality

$$\Delta(e\Phi) = e\Delta V_{WR} \qquad [5]$$

established both theoretically (9–10, 43–44) and experimentally (45–46). A decrease in the work function ($\Delta(e\Phi) < 0$) results in the enhancement of the rates of formation of N_2, N_2O, and CO_2 and thus the system exhibits electrophilic behavior (9). A modification of the selectivity toward nitrogen is also observed with an increase of S_{N_2} from a value of 0.22 under open-circuit conditions to 0.35 when $\Delta(e\Phi) = -1.3$ eV. No effect on the reaction rate or selectivity is observed for a positive increase of the work function. The rate enhancement ratio ρ is defined as

$$\rho = r/r^0 \qquad [6]$$

Rate enhancement ratios of $\rho_{CO_2} = 2.1$, $\rho_{N_2O} = 1.5$, and $\rho_{N_2} = 3.1$ are measured for $V_{WR} = -1.6$ V.

Exchange Current Measurements

Exchange current values of $I_{0,c} = 0.13\ \mu A$ and $I_{0,a} = 0.09\ \mu A$ were extracted under catalytic reaction conditions from the linear (Tafel) part of the log I vs η curves (Fig. 5) for anodic ($I > 0$) and cathodic ($I < 0$) operation. From the slopes of the linear ln I vs η lines, one obtains $\alpha_a = 0.2$ and $\alpha_c = 0.17$ for the anodic and cathodic transfer coefficient,

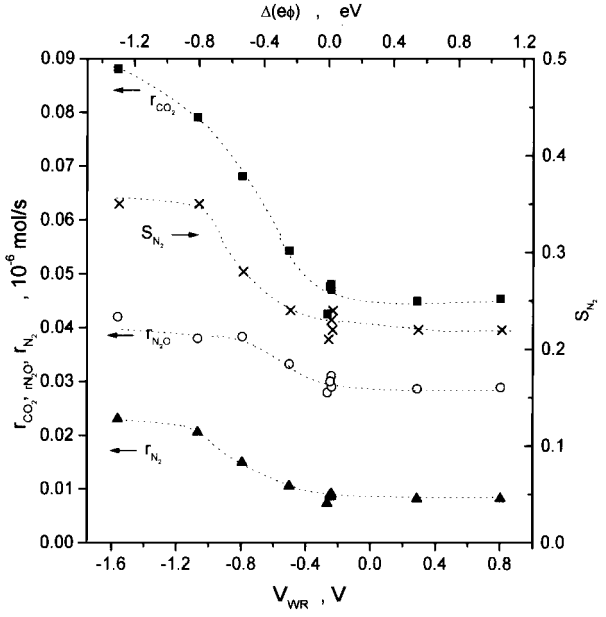

FIG. 4. Effect of the catalyst potential (V_{WR}) on the CO_2, N_2, N_2O formation rates and the selectivity of NO reduction to N_2. Conditions: $T = 646$ K, $P^0_{NO} = 1.34$ kPa, $P^0_{CO} = 0.55$ kPa.

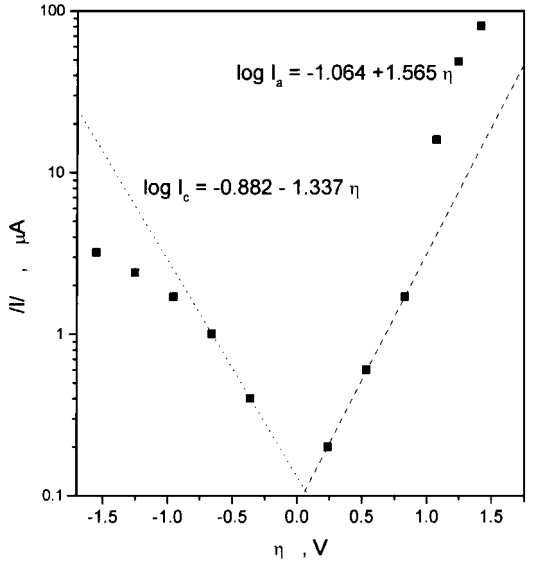

FIG. 5. Dependence of anodic ($I > 0$) and cathodic ($I < 0$) current on catalyst overpotential. Conditions: $T = 646$ K, $P^0_{NO} = 1.34$ kPa, $P^0_{CO} = 0.55$ kPa.

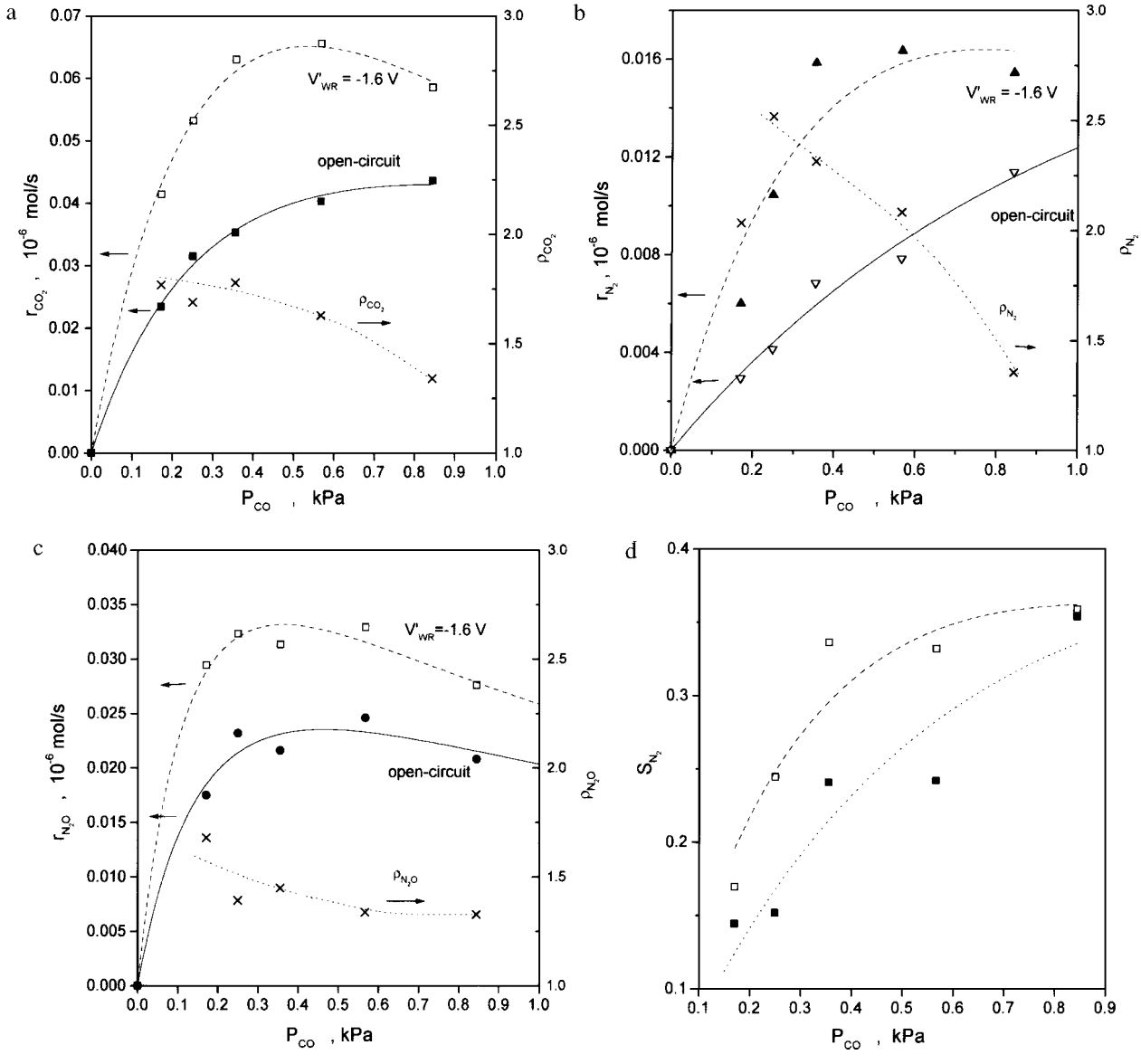

FIG. 6. Effect of the partial pressure of CO (P_{CO}) on the rates of CO_2 (a), N_2 (b), and N_2O (c) formation, and on the selectivity of NO reduction to N_2 (d) for open-circuit and $V'_{WR} = -1.6$ V. Conditions: $T = 646$ K, $P_{NO} = 1.3$ kPa.

respectively. It is interesting to note that a limiting current behavior is observed for the cathodic curve where the NEMCA effect was observed. Oxygen dissolution and diffusion in the Pd catalyst, similarly as observed for Ag catalysts (47) could be responsible for this effect. The limiting current must also reflect a very low surface concentration of adsorbed oxygen on the catalyst during the CO + NO reaction.

Effect of P_{CO} and P_{NO} on the Open- and Close-Circuit Steady-State Rates

The dependence of the CO_2, N_2, and N_2O rates and of selectivity S_{N_2} on P_{CO} at fixed P_{NO} under open-circuit conditions and for $V'_{WR} = -1.6$ V is shown in Figs. 6a, b, c, d for $T = 646$ K. Langmuir–Hinshelwood type curves are obtained which do not evidence a strong inhibition by carbon monoxide in the partial pressure range studied. The rate enhancement ratio ρ decreases with increasing values of P_{CO}, indicating that the electrochemical promotion effect becomes less effective as P_{CO} increases. The corresponding S_{N_2} data are shown in Fig. 6d. The selectivity toward nitrogen increases with P_{CO}. It is also apparent that higher selectivities are always obtained under closed-circuit conditions.

Figures 7a, b, c, and d show the corresponding results for the dependence of r_{CO_2}, r_{N_2}, r_{N_2O}, and S_{N_2} on P_{NO} at

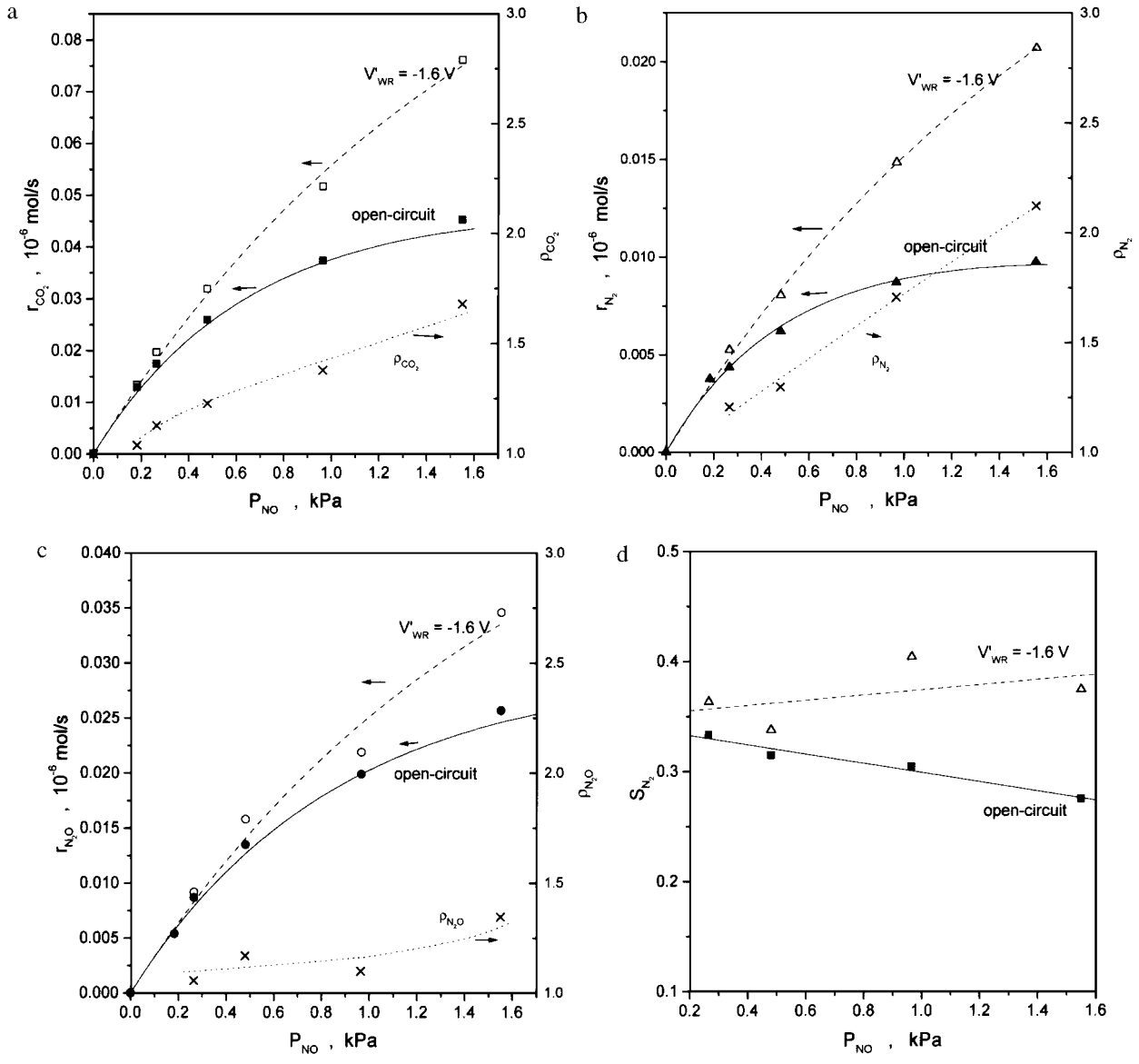

FIG. 7. Effect of the partial pressure of NO (P_{NO}) on the rates of CO_2 (a), N_2 (b), and N_2O (c) formation, and on the selectivity of NO reduction to N_2 (d) for open-circuit and $V'_{WR} = -1.6$ V. Conditions: $T = 646$ K, $P_{CO} = 0.5$ kPa.

fixed P_{CO}. The extent of the electrochemical promotion increases almost linearly with P_{NO}. As also observed in Fig. 6, negative potentials always result in an increase of S_{N_2}.

An apparent activation energy of 73 kJ/mol was measured between 603 K and 743 K under open-circuit conditions for an outlet gas composition of $P_{CO} = 0.55$ kPa and $P_{NO} = 1.3$ kPa (Fig. 8). This value is lower than values of 85 to 91 kJ/mol reported in the literature (28, 29, 31). A limitation by external mass transfer was discarded, since the rate was measured to be constant, within experimental error, when the flow rate was varied by a factor of 3. It is worth noting that the selectivity towards N_2 was also measured to be constant as the flow rate was varied. This strongly suggests a parallel rather than consecutive route for the production of N_2 and N_2O.

$N_2O + CO$ Reaction

The steady-state CO_2 production rate dependence on P_{CO} and P_{N_2O} at respectively fixed P_{N_2O} and P_{CO} values under open-circuit conditions is shown in Fig. 9 for a temperature of 673 K. The rate is first-order in N_2O and negative order in CO, which evidences a strong site blocking by carbon monoxide. A comparison of r_{CO_2} for the $CO + N_2O$, $CO + NO$, and $CO + O_2$ reactions, extrapolated at 673 K is shown in Table 1, together with the apparent activation energy values used for the extrapolation. Relative

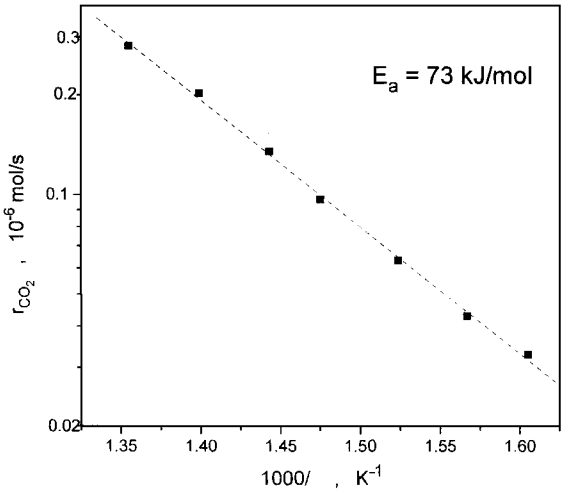

FIG. 8. NO + CO reaction: Arrhenius plot of the rate of CO_2 formation under open-circuit conditions; $P_{CO} = 0.55$ kPa, $P_{NO} = 1.3$ kPa.

CO_2 production rate increase in the order CO + N_2O [1], CO + NO [7], and CO + O_2 [1.48×10^4].

Galvanostatic transient experiments are shown in Fig. 10 for a constant current imposition of I = 200 μA and I = −300 μA. Both electrophobic and electrophilic behavior is observed as the rate is enhanced with the application of both positive and negative currents, respectively. The catalytic rate increases by a factor of $\rho = 1.7$ for I = −300 μA and $\rho = 1.4$ for I = 200 μA. In both cases the increase

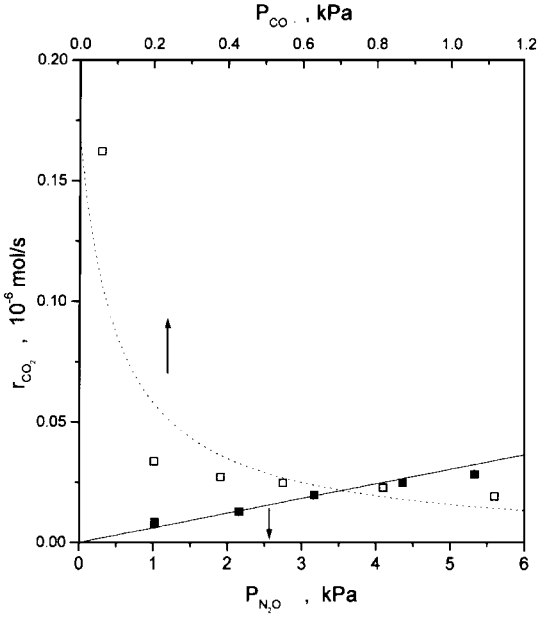

FIG. 9. N_2O + CO reaction: effect of the partial pressure of N_2O (P_{N_2O}) on the rate of CO_2 formation at a constant $P_{CO} = 0.55$ kPa (solid line, bottom axis) and of the partial pressure of CO (P_{CO}) on the rate of CO_2 formation at a constant $P_{N_2O} = 4.4$ kPa (dotted line, top axis). Conditions: $T = 673$ K.

TABLE 1

Comparison of r_{CO_2} for the CO + N_2O, CO + NO, and CO + O_2 Reactions

Reaction	T [K]	P_{CO} [kPa]	P_{ox} [kPa]	r_{CO_2} [10^{-7} mol/s]	[a] $r_{CO_2,673\ K}$ [10^{-7} mol/s]	Ratio
CO + N_2O	673	0.55	1.55	0.107	0.107	1
CO + NO	646	0.55	1.55	0.452	0.784	7
CO + O_2	498	0.75	1.00	0.419	1587	1.48×10^4

[a] Calculated using $E_a = 73.7$ kJ/mol for CO + NO and $E_a = 131.2$ for CO + O_2.

of the rate is approximately 20 times larger the transport of O^{2-} to or from the catalyst, I/2F, calculated from Faraday's law.

The steady-state CO_2 production rate is presented in Fig. 11 as a function of the ohmic drop free catalyst potential V_{WR} at 673 K for a constant inlet pressure of the reactants $P^0_{N_2O} = 4.8$ kPa and $P^0_{CO} = 0.52$ kPa. The top axis of the figure is based on Eq. [5]. The reaction exhibits inverse-volcano type behavior (10).

DISCUSSION

NO + CO Reaction

The present work demonstrates that on Pd interfaced with YSZ, the application of an external negative potential results in the enhancement of both the catalytic rate of reduction of CO by NO and of the selectivity of the reaction towards N_2. The effect is non-Faradaic; that is, the modification of the rate is typically more than 700 times larger than

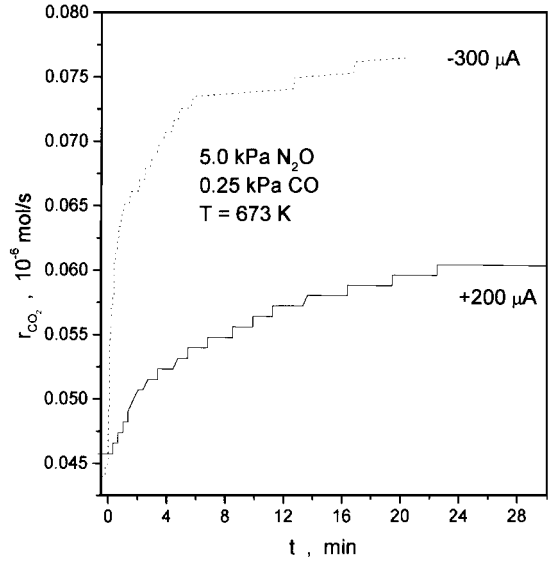

FIG. 10. N_2O + CO reaction: galvanostatic transient showing the effect of a step change of the applied current of I = −300 μA (dotted line) and I = 200 μA (solid line) on the CO_2 formation. Conditions: $T = 673$ K, $P^0_{N_2O} = 5.0$ kPa, $P^0_{CO} = 0.25$ kPa.

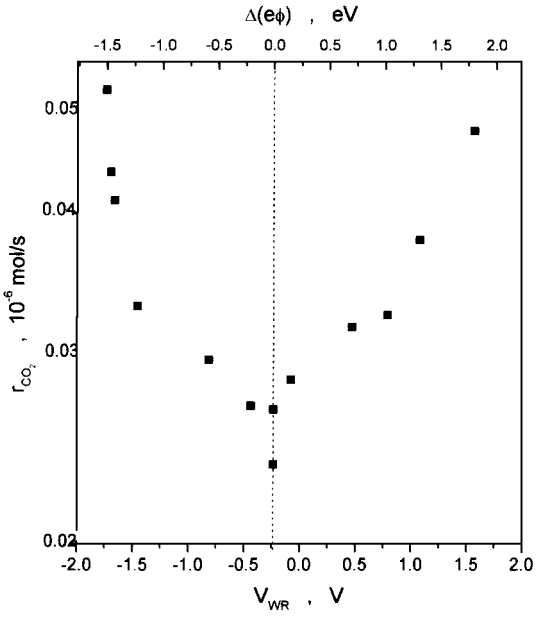

FIG. 11. $N_2O + CO$ reaction: effect of the catalyst potential (V_{WR}) on the rate of CO_2 formation. Conditions: $T = 673$ K, $P^0_{N_2O} = 4.8$ kPa, $P^0_{CO} = 0.52$ kPa.

the rate of transport of O^{2-} through the solid electrolyte and is related to a change of the work function of the metal. Similarly to the cases of the Na-promoted Pt-catalyzed NO reduction by CO (11) or H_2 (14), these observations can be rationalized by an enhanced adsorption and dissociation of NO as the potential and the work function (45) of the catalyst surface is decreased. The similarity of the trends obtained with two different solid electrolytes and therefore different promoting species (Na^+ or $O^{\delta-}$) is one more indication of the validity of the theoretical explanation proposed for the NEMCA phenomenon (9–10). The situation is slightly more complex in the case of the $CO + NO$ reaction than in the cases of the $NO + H_2$, $NO + C_2H_4$, or $C_2H_4 + O_2$ systems because in the present case both CO and NO can have a similar type of chemisorptive bonding to the metal surface (Blyholder model) and both have been found to act predominantly as electron acceptor adsorbates (10, 11). A decrease of the work function should therefore enhance the adsorption of both species, and the resulting modification of the reaction rate will depend on the relative strength of adsorption of the two adsorbates as well as on the relative effect of the work function decrease on the chemisorptive binding strength of the two species. For Pt, a decrease of the work function results in an enhanced adsorption of NO compared to CO, as is evidenced by a shift of the P_{CO} values which maximize the rate, P^*_{CO}, toward larger values as the work function decreases (11). An opposite trend is observed for Pd (Figs. 5a, b, c), as the different rates reach a maximum as P_{CO} is increased under closed-circuit conditions, while no maximum is observed under open-circuit conditions. This difference is thought to result from the different relative binding strength of CO and NO on Pd and Pt, which is evidenced by the different kinetic behaviors. A strong inhibition of CO was shown for Pt (11) but it is not observed for Pd (Figs. 5a, b, c). The higher rate enhancement ratios observed on Pt resulted from the concomitant shift of P^*_{CO} and of the rate maximum to higher values. Only the latter effect is taking place in the case of Pd and thus the lower rate enhancement ratios observed. A direct comparison between two different metals as to the extent of the NEMCA effect can, however, be misleading, as, for example, rate enhancement ratios of up to 60 have been measured for the complete oxidation of ethylene on Pt interfaced with YSZ (43) while factors of 1.5 have been measured for the same reaction on Pd (48).

The extent of the electrochemical promotion effect is dependent on the gaseous composition. The rate enhancement ratios increase with P_{NO} (Figs. 7a, b, c) but decrease with P_{CO} (Figs. 6a, b, c). These figures show clearly that CO adsorption is enhanced *relatively* to NO on Pd as the catalyst potential and work function is decreased. This is manifest by the appearance of a rate maximum with respect to P_{CO} (Fig. 6) and by the observed increase in apparent rate order with respect to P_{NO} (Fig. 7). On the other hand, since both CO and NO are expected to behave predominantly as electron acceptors (10, 11) it is anticipated that the chemisorptive bond strength of both will be strengthened with decreasing potential and work function, although the relative effect is in the present case more pronounced for CO. Increasing chemisorptive binding strength of NO will cause an enhanced degree of NO dissociation and this is consistent with the observed enhancement of product selectivity towards N_2 with decreasing catalyst potential and work function (Figs. 6d and 7d). According to the unimolecular mechanism discussed below, enhanced NO dissociation should also significantly enhance the NO reduction rate under conditions where the number of empty sites is significant, i.e., under conditions where the coverage of the more strongly bonded CO is lower. This can explain why the electrochemical promotion effect diminishes for high P_{CO}/P_{NO} ratios (Figs. 6 and 7).

Two reaction schemes are proposed for the reduction of NO by CO on Pd. The unimolecular mechanism (e.g., (30, 32)) involves the dissociation of NO to form adsorbed atomic nitrogen and oxygen, the latter being scavenged by CO, while in the bimolecular scheme (e.g., (16, 29, 31)) CO and NO react prior to the dissociation of NO:

Unimolecular:

$$CO + S \leftrightarrow CO_a \quad [7]$$

$$NO + S \leftrightarrow NO_a \quad [8]$$

$$NO_a + S \leftrightarrow N_a + O_a \quad [9]$$

$$N_a + N_a \rightarrow N_2 + 2S \quad [10]$$

$$N_a + NO_a \rightarrow N_2O + 2S \quad [11]$$

$$CO_a + O_a \rightarrow CO_2 + 2S. \quad [12]$$

Bimolecular: [9] and [12] are replaced by

$$NO_a + CO_a \leftrightarrow N_a + CO_2 + S. \quad [13]$$

Whether considering a unimolecular or bimolecular pathway, the two reactions controlling the selectivity towards N_2 are [10] and [11]. The ratio of these two reactions is equal to

$$r_{10}/r_{11} = S_{N_2}/(1 - S_{N_2}) = (k_{10}\theta_N)/(k_{11}\theta_{NO}) = k'(\theta_N/\theta_{NO}). \quad [14]$$

If it is assumed that neither k_{10} nor k_{11} vary significantly with P_{CO}, P_{NO}, or $\Delta(e\phi)$, then the change of $S_{N_2}/(1-S_{N_2})$ with these parameters directly reflects the variation of θ_N/θ_{NO}.

A significant increase in this ratio is observed in Fig. 12a with increasing P_{CO}. This can be immediately rationalized on the basis of the unimolecular mechanism as follows: Since step [9] is in equilibrium, the coverages of NO, N, O and the surface sites, θ_{NO}, θ_N, θ_O, and θ_v, respectively, are related via

$$\theta_N/\theta_{NO} = (K\theta_v)/\theta_O, \quad [15]$$

where K is an equilibrium constant. It should be noted that K relates surfaces coverages, not gaseous activities, and thus, its value is expected to depend not only on temperature but also on catalyst potential. The variation of adsorption equilibrium constants with catalyst potential is well documented (10, 54). As previously noted decreasing catalyst potential and work function is expected to enhance NO dissociation and thus increase K which is consistent with the observed increase in $S_{N_2}/(1-S_{N_2})$, thus in θ_N/θ_{NO} with negative applied potentials (Fig. 12a). Furthermore, Eq. [15] is consistent with the observed increase in $S_{N_2}/(1-S_{N_2})$, thus in θ_N/θ_{NO} with increasing P_{CO} (Fig. 12a). An increase in P_{CO} will decrease θ_O, thus causing an increase in the θ_N/θ_{NO} ratio (Eq. [15]) and thus on S_{N_2} (Eq. [14]) as experimentally observed both for open-circuit and for negative applied potentials (Fig. 12a).

Equation [15] can also explain the observed dependence of $S_{N_2}/(1-S_{N_2})$, thus of θ_N/θ_{NO} on P_{NO} (Fig. 12b). Increasing P_{NO}, at fixed P_{CO}, causes a decrease in θ_v and a concomitant increase in θ_O, both consistent with the observed decrease in the θ_N/θ_{NO} ratio with increasing P_{NO} under open-circuit conditions (Eq. [15] and Fig. 12b). Negative current and potential application causes an increase in K and a concomitant decrease in θ_O, both consistent with the observed enhancement in the θ_N/θ_{NO} ratio under negative potentials (Fig. 12b). Increasing P_{NO} has now a lesser effect on θ_O which is governed primarily by the rate of electrochemical oxygen removal, I/2F, thus the decreasing effect of P_{NO} on the θ_N/θ_{NO} ratio practically vanishes (Fig. 12b).

Consequently all the observed kinetic trends are in qualitative agreement with the unimolecular mechanism and with enhanced NO dissociation with decreasing potential as in previous electrochemical NO reduction studies (11–14).

$N_2O + CO$ Reaction

The study of the electrochemical promotion effect on the $N_2O + CO$ reaction was motivated by the fact that

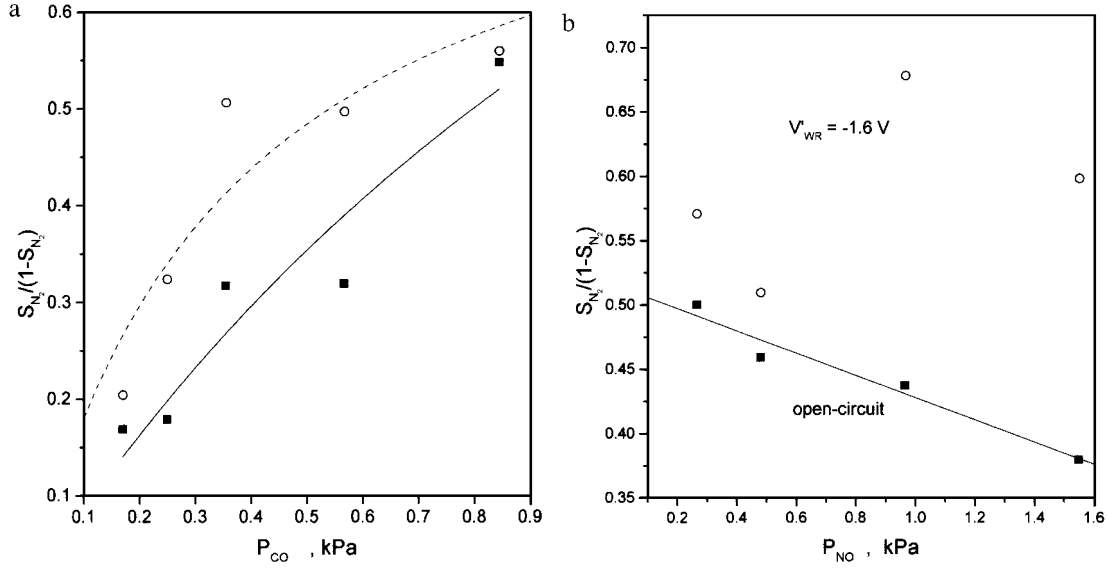

FIG. 12. NO + CO reaction: effect of the partial pressure of CO (a) and NO (b) on the ratio $S_{N_2}/(1 - S_{N_2})$ for open-circuit and $V'_{WR} = -1.6$ V. Conditions: $T = 646$ K, $P_{NO} = 1.3$ kPa (a), and $P_{CO} = 0.5$ kPa (b).

both of these reactants are present in the gas phase during the CO + NO reaction. A brief kinetic study shows that at 673 K, a strong inhibition by CO is observed, as evidenced by a drastic decrease of the rate with P_{CO} and a linear increase with P_{N_2O} (Fig. 9). A comparison of the rates of CO_2 production for the $CO + N_2O$ and CO + NO reactions shows a relative ratio of respectively 1 to 7 (673 K, $P_{CO} = 0.55$ kPa, $P_{NO} = P_{N_2O} = 1.55$ kPa, Table 1). While such comparison was not found in the literature for Pd, Mc Cabe and Wong (33) report relative turnover numbers for a supported Rh catalyst of $CO + N_2O$ [1], CO + NO [710], and $CO + O_2$ [4.4×10^5], for stoichiometric mixtures extrapolated to 475 K. Our result is surprising in the sense that according to the Pt > Pd > Rh order of strength of CO adsorption (22) one would expect a stronger inhibition of CO on Pd than on Rh for the $CO + N_2O$ reaction and therefore reversed trends. This may be explained if the sticking coefficient of N_2O on Pd is larger than on Rh.

The relative rate difference between the $CO + N_2O$ and CO + NO on Pd further decreases if r_{N_2} instead of r_{CO_2} is considered. Assuming $S_{N_2} = 0.3$ at 673 K for the CO + NO reaction, a respective ratio of 1 to 1.6 is obtained. This comparison is, however, not realistic since a $P_{N_2O} = 0.02$ kPa and not 1.55 kPa is measured during the CO + NO reaction. Assuming a linear dependence of r_{N_2O} on P_{N_2O} (Fig. 9), the ratio then becomes 1 to 124.

Cho (35, 49) has, however, shown that such comparisons can be very misleading and that dramatic differences can exist if $N_2O + CO$ is considered as an intermediate or as an isolated reaction. The observed constancy of the selectivity toward N_2 as the flowrate is increased by a factor of 3 allows us, however, to conclude that this reaction is not an important subreaction in the CO + NO system.

An enhancement of r_{N_2O} is observed upon the application of both negative and positive external potentials. N_2O is known to dissociate on metal surfaces by nitrogen–oxygen bond cleavage which releases N_2 directly in the gas phase and leaves a strongly adsorbed atomic oxygen (33). The electrophilic behavior is attributed to an enhanced N_2O dissociation as the work function is decreased while the electrophobic behavior is attributed to a decrease of the CO inhibition as the work function is increased. The relatively small rate enhancement ratios observed show that the $N_2O + CO$ reaction is not responsible for the observed rate enhancements of the CO + NO reaction.

Time Constants

The NEMCA time constant τ is defined as the time required for the rate Δr to reach 63% of its steady-state value during a galvanostatic transient. A general observation in NEMCA studies with O^{2-} conductors is that the magnitude of τ can be predicted from $\tau \sim 2FN_O/I$, where N_O corresponds to the reactive oxygen uptake of the catalyst (9, 10). Table 2 compares the values of τ and $2FN_O/I$ obtained in the galvanostatic transients presented in Figs. 2 and 8. A good correspondence is obtained for the $CO + N_2O$ reaction for the application of a positive current. However, for both the $CO + N_2O$ and CO + NO reactions the time constants measured with negative currents are respectively one and two orders of magnitude smaller than $2FN_O/I$.

TABLE 2

Measured τ and Predicted $2FN_O/I$ Values

Reaction	Current [μA]	τ [min]	$2FN_O/I$ [min]
CO + NO	−10	2.9	292.7
$CO + N_2O$	−300	0.9	10.7
$CO + N_2O$	+200	11.2	14.6

The change of the catalytic rate is related to the change of the work function of the catalyst through an exponential relationship (9, 10). For the work function to change, the coverages and/or dipole moments of species already adsorbed on the surface must change, or new species must get adsorbed. It is now firmly established that the change in the work function for a positive current is predominantly due to the migration of $O\delta^-$ originating from the solid electrolyte (50–54). $2FN_O/I$ expresses then the time required to form a monolayer of $O^{\delta-}$ on the metal surface.

Such species are, however, not formed during the application of negative currents and, thus, the work function change must be generated by a modification of the surface coverages and dipole moments of the species already adsorbed on the catalyst. A correspondence between $2FN_O/I$ and τ, as has been measured, for example, during the $CO + O_2$ reaction (55) is more difficult to explain, but it can be accounted for by the fact that the surface coverage of oxygen is high and of the order of 0.2–1. The discrepancy between τ and $2FN_O/I$ measured in this work shows that the number of sites implicated in the change of work function is one to two orders of magnitude smaller than N_O. During the application of a constant negative current, O_a diffuses to the three-phase boundary (tpb), where the electrochemical charge transfer reaction takes places. If it is assumed that it is the changing coverage of O_a which is primarily responsible for the change in the catalyst work function, then a decrease of the surface concentration of this species should lead to a more negative potential. A coverage of O_a one to two orders of magnitude smaller than N_O seems reasonable for these reactions, where O_a is formed by the dissociation of N_O or N_2O and is rapidly scavenged by carbon monoxide, as is shown in Table 1 by the comparatively much higher rate of the $CO + O_2$ reaction. Consequently the ratio $\tau/(2FN_O/I)$ may provide a measurement of the very low coverage of atomic oxygen on the catalyst surface at the start of the galvanostatic transient.

CONCLUSIONS

The catalytic activity of Pd for the reduction of NO by CO can be reversibly affected via electrochemical promotion. The effect is more pronounced as P_{NO} is increased or P_{CO} decreased. In the most favorable case, the rates of CO_2 and N_2 production are respectively doubled and tripled. Under all conditions, the selectivity towards N_2 versus N_2O increases as the catalyst work function is decreased. These observations strongly support the view that decreasing the work function of the catalyst enhances the NO dissociation rate on Pd but that the overall promoting effect is moderated by a stronger adsorption of CO relative to NO.

The $N_2O + CO$ reaction rate also exhibits NEMCA behavior, with an observed twofold enhancement of the rate in the most favorable case as the work function is either increased or decreased. The N_2 formation rate is in the same order of magnitude as for the $NO + CO$ reaction when $P_{N_2O} = P_{NO}$. It is, however, concluded that this reaction is not an important route to the formation of N_2 during the $NO + CO$ reaction under the present conditions.

ACKNOWLEDGMENTS

We thank the EEC JOULE and HCM programs and the EPET II program of the Hellenic Secretariat of Research and Technology for financial support.

Note added in proof: In a recent communication (56) Haller and Kim studied the electrochemical promotion of the same catalytic system. Their results, and in particular the measured Λ and ρ values, are in good qualitative agreement with this work.

REFERENCES

1. Taylor, K. C., *Catal. Rev.-Sci. Eng.* **35**(4), 457 (1993).
2. Shelef, M., and Graham, G. W., *Catal. Rev.-Sci. Eng.* **36**(3), 433 (1994).
3. Summers, J. C., and Williamson, W. B., ACS Symp. Ser., Vol. 55 (J. N. Armor, Ed.), Am. Chem. Soc., Washington, DC, 1994.
4. Dettling, J., Hu, Z., Lui, Y. K., Smaling, R., Wan, C. Z., and Punke, A., *Stud. Surf. Sci. Catal.* **96**, 461 (1995).
5. Papadakis, V. G., Pliangos, C. A., Yentekakis, I. V., Verykios, X. E., and Vayenas, C. G., *Catal. Today* **29**, 71 (1996).
6. Gandhi, H-S., Yao, H. C., and Stepien, H. K., ACS Symp. Ser., Vol. 178, p. 143, Am. Chem. Soc., Washington, DC, 1982.
7. Muraki, H., Shinjoh, H., Sobukawa, H., Yokota, K., and Fujitani, Y., *Ind. Eng. Chem. Prod. Res. Dev.* **25**, 202 (1986).
8. Muraki, H., Yokota, K., and Fujitani, Y., *Appl. Catal.* **48**, 93 (1989).
9. Vayenas, C. G., Bebelis, S., Yentekakis, I. V., and Lintz, H.-G., *Catal. Today* **11**, 303 (1992).
10. Vayenas, C. G., Jaksic, M. M., Bebelis, S. I., and Neophytides, S. G., The electrochemical activation of catalytic reactions, *in* "Modern Aspects of Electrochemistry" (J. O.'M. Bockris, B. E. Conway, and R. E. White, Eds.), Vol. 29, pp. 57–202, Plenum, New York, 1996.
11. Palermo, A., Lambert, R. M., Harkness, I. R., Yentekakis, I. V., Mar'ina, O., and Vayenas, C. G., *J. Catal.* **161**, 471 (1996).
12. Harkness, I. R., and Lambert, R. M., *J. Catal.* **152**, 211 (1995).
13. Lambert, R. M., Tikhov, M., Palermo, A., Yentekakis, I. V., and Vayenas, C. G., *Ionics* **1**, 366 (1995).
14. Mar'ina, O. A., Yentekakis, I. V., Vayenas, C. G., Palermo, A., and Lambert, R. M., *J. Catal.* **166**, 218 (1997).
15. Xu, X., and Goodman, D. W., *Catal. Lett.* **24**, 31 (1994).
16. Davies, P. W., and Lambert, R. M., *Surf. Sci.* **110**, 227 (1981).
17. Schmick, H.-D., and Wassmuth, H.-W., *Surf. Sci.* **123**, 471 (1982).
18. Ramsier, R. D., Gao, Q., Waltenburg, H. N., and Yates, Jr., J. T., *J. Chem. Phys.* **100**(9), 6837 (1994).
19. Conrad, H., Ertl, G., Kuppers, J., and Latta, E. E., *Surf. Sci.* **65**, 235 (1977).
20. Moriki, S., Inoue, Y., Miyazaki, E., and Yasumori, I., *J. Chem. Soc. Faraday Trans. 1* **78**, 171 (1982).
21. Obuchi, A., Naito, S., Onishi, T., and Tamaru, K., *Surf. Sci.* **122**, 235 (1982).
22. Muraki, H., and Fujitani, Y., *Ind. Eng. Chem. Prod. Res. Dev.* **25**, 414 (1986).
23. Yamada, T., Matsuo, I., Nakamura, J., Xie, M., Hirano, H., Matsumoto, Y., and Tanaka, K.-I., *Surf. Sci.* **231**, 303 (1990).
24. Alikina, G. M., Davydov, A. A., Sazanova, I. S., and Popovskii, V. V., *Kinet. i Katal.* **28**(2), 418 (1987).
25. Alikina, G. M., Davydov, A. A., Sazanova, I. S., and Popovskii, V. V., *Kinet. i Katal.* **28**(3), 655 (1987).
26. Daté, M., Okuyama, H., Takagi, N., Nishijima, M., and Aruga, T., *Surf. Sci.* **341**, L1096 (1995).
27. Xu, X., Peijun, C., and Goodman, D. W., *J. Phys. Chem.* **98**, 9242 (1994).
28. Graham, G. W., Logan, A. D., and Shelef, M., *J. Phys. Chem.* **97**, 21, 5445 (1993).
29. Butler, J. D., and Davis, D. R., *J. Chem. Soc. Dalton Trans.*, 2249 (1976).
30. Muraki, H., Shinjoh, H., and Fujitani, Y., *Ind. Eng. Chem. Prod. Res. Dev.* **25**, 419 (1986).
31. Xi, G., Bao, J., Shao, S., and Li, S., *J. Vac. Sci. Technol. A* **10**(4), 2351 (1992).
32. Bogdanchikova, N. E., Boreskov, G. V., and Khasin, A. V., *Kinet. i Katal.* **21**(6), 1501 (1980).
33. McCabe, R., and Wong, C., *J. Catal.* **121**, 422 (1990).
34. Belton, D. N., and Schmieg, S. J., *J. Catal.* **138**, 70 (1992).
35. Cho, B. K., *J. Catal.* **148**, 697 (1994).
36. Adlhoch, W., Kohler, R., and Lintz, H. G., *Z. Phys. Chem. N. F.* **120**, 111 (1980).
37. Sadhankar, R. R., Ye, J., and Lynch, D. T., *J. Catal.* **146**, 511 (1994).
38. Yentekakis, I. V., and Bebelis, S., *J. Catal.* **137**, 278 (1992).
39. Stoukides, M., and Vayenas, C. G., *J. Catal.* **64**, 18 (1980).
40. Peuckert, M., *J. Phys. Chem.* **89**, 2481 (1985).
41. Rodriguez, N. M., Oh, S. G., Dalla-Betta, R. A., and Baker, R. T. K., *J. Catal.* **157**, 676 (1995).
42. Chen, J. J., and Ruckenstein, E., *J. Phys. Chem.* **85**, 1606 (1981).
43. Bebelis, S., and Vayenas, C. G., *J. Catal.* **118**, 125 (1989).
44. Neophytides, S., and Vayenas, C. G., *J. Catal.* **118**, 147 (1989).
45. Vayenas, C. G., Bebelis, S., and Ladas, S., *Nature (London)* **343**(6259), 625 (1990).
46. Ladas, S., Bebelis, S., and Vayenas, C. G., *Surf. Sci.* **251/252**, 1062 (1991).
47. Bebelis, S., and Vayenas, C. G., *J. Catal.* **138**, 588 (1992).
48. Bebelis, S., Vayenas, D., and Yiokari, K., *Catal. Lett.*, submitted.
49. Cho, B. K., *J. Catal.* **138**, 255 (1992).
50. Arakawa, T., Saito, A., and Shiokawa, J., *Appl. Surf. Sci.* **16**, 365 (1983).
51. Zipprich, W., Wiemhofer, H.-D., Vohrer, U., and Gopel, W., *Ber. Bunsenges. Phys. Chem.* **94**, 1406 (1995).
52. Ladas, S., Kennou, S., Bebelis, S., and Vayenas, C. G., *J. Phys. Chem.* **97**, 8845 (1993).
53. Jiang, Y., Yentekakis, I. V., and Vayenas, C. G., *J. Catal.* **148**, 240 (1994).
54. Neophytides, S., and Vayenas, *J. Phys. Chem.* **99**, 17063 (1995).
55. Yentekakis, I. V., and Vayenas, C. G., *J. Catal.* **111**, 170 (1988).
56. Haller, G. L., and Kim, S., ACS Petroleum Division Preprints, Symposium on Catalytic Combustion, 213th National ACS Meeting, San Fransisco, CA, April 13–17, 1997, pp. 155–158.